AD NUMBER

AD831898

LIMITATION CHANGES

TO:

Approved for public release; distribution is unlimited.

FROM:

Distribution authorized to U.S. Gov't. agencies and their contractors; Critical Technology; APR 1968. Other requests shall be referred to Army Electronics Command, AMSEL-KL-SM, Fort Monmouth, NJ. This document contains export-controlled technical data.

AUTHORITY

usaec ltr, 30 jul 1971

AD

TECHNICAL REPORT ECOM-0671-2

MICROWAVE GENERATION FROM AVALANCHE TRANSIT TIME DIODES

SECOND QUARTERLY REPORTS

by

A.H. Solomon
C.A. Levi
E.F. Scherer

APRIL, 1968

ECOM

UNITED STATES ARMY ELECTRONICS COMMAND • FORT MONMOUTH, N.J.

The work prepared under this contract is a part of PROJECT DEFENDER and was made possible by the support of the Advanced Research Projects Agency under Order Number 692, through the U.S. Army Electronics Command.
Contract No. DAAB07-67-C-0671

Contract No.

SYLVANIA
SYLVANIA ELECTRIC PRODUCTS INC.
Subsidiary of GENERAL TELEPHONE & ELECTRONICS
SEMICONDUCTOR DIVISION
100 Sylvan Road • Woburn, Mass. 01801

NOTICES

DISCLAIMERS

The findings in this report are not to be construed as an official Department of the Army position, unless so designated by other authorized documents.

The citation of trade names and names of manufacturers in this report is not to be construed as official Government indorsement or approval of commercial products or services referenced herein.

DISPOSITION

Destroy this report when it is no longer needed. Do not return it to the originator.

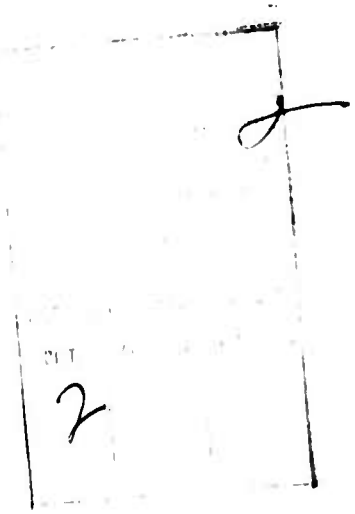

REPORTS CONTROL SYMBOL
OSD 1366

TECHNICAL REPORT ECOM-0671-2 APRIL, 1968

MICROWAVE GENERATION FROM AVALANCHE TRANSIT TIME DIODES

SECOND QUARTERLY REPORT

1 OCTOBER 1967 TO 31 DECEMBER 1967

Report No. 2

CONTRACT NO. DAAB07-67-C-0671

DA PROJECT NO. 7910.21.243.38

Prepared by:

A. H. Solomon
C. A. Levi
E. F. Scherer

Sylvania Electric Products, Inc.
SEMICONDUCTOR DIVISION
Woburn, Massachusetts

The work prepared under this contract is part of PROJECT DEFENDER and was made possible by the support of the Advanced Research Projects Agency under Order Number 692, through the U.S. Army Electronics Command

for

U.S. ARMY ELECTRONICS COMMAND, FORT MONMOUTH, NEW JERSEY

ABSTRACT

Work during the second quarter was devoted to device geometry optimization, inverted chip mounting, diamond heat sink classification and evaluation of noise characteristics. While inverted chip mounting was effective in reducing thermal resistance, oscillator efficiency was lower than that obtained from similar devices conventionally mounted. Several possible reasons for the poor RF performance of inverted chip diodes are being investigated. However, conventionally-mounted devices were pulse tested and over 1 watt of peak pulse power was obtained at 8.6 GHz, with 7 percent efficiency. These diodes are being studied as models of desired characteristics in inverted mount devices. Noise measurements on various diodes indicate that AM noise is essentially constant from about 100 MHz off carrier down to 200 Hz off carrier, which is as close to the carrier as measurements could be made. The sideband noise-to-carrier ratio was about -105 db in a 1 KHz bandwidth, in an oscillator cavity having a loaded Q of about 100.

FOREWORD

This program is a research and development effort designed to investigate avalanche transit time-generated oscillations in semiconductor devices, with the objective being the design and construction of avalanche transit time oscillators capable of delivery at least ten watts CW output power. The work prepared under this contract is a part of PROJECT DEFENDER and was made possible by the support of the Advanced Research Projects Agency under Order Number 692, through the U. S. Army Electronics Command.

This report was prepared by Arthur H. Solomon, Head of the Solid State Circuits Development Section of Sylvania's Semiconductor Division, with the assistance of C. Levi, W. K. Niblack, E. Scherer and W. Landry of the Sylvania Semiconductor division, and R. I. Harrison of General Telephone and Electronics Laboratories, Inc.

TABLE OF CONTENTS

LIST OF FIGURES

LIST OF TABLES

BLANK PAGE

I. INTRODUCTION AND SUMMARY

This program is a research and development effort to investigate avalanche transit time-generated oscillations in semiconductor junctions. Objectives include the investigation of semiconductor materials and junction techniques leading to the design and constructuion of avalanche transit time oscillators capable of delivering at least ten watts of CW output power. In addition, a pulsed device capable of at least 100 watts peak power output will also be developed. The approach to device development for high power will include the design of multi-junction diodes on a common high-thermal-conductivity substrate. Power combining techniques for paralleling many oscillators and/or amplifiers will also be investigated, with an ultimate objective of producing power outputs at a kilowatt level. Emphasis will also be placed upon tunability, gain, bandwidth, efficiency, noise characteristics, reliability, stability, uniformity, reproducibility and cost.

I. 1 Program Goals

The overall goals of this program are:

1. Develop avalanche transit time diode oscillators capable of at least 10 watts CW power and 100 watts peak pulse power in the 1 - 12 GHz frequency range, with emphasis on C-band. No forced air or other external cooling means is to be employed.

2. Develop techniques for combining the outputs of many such oscillators to achieve higher output.

3. Develop techniques for frequency stabilization, noise reduction and wideband mechanical and electronic tuning.

I. 2 Results Obtained During the Second Quarter

Considerable effort was expended during this period on investigation of device geometries for high CW power, and on inverted mounting of diodes. A number of inverted mount diodes were fabricated, but none gave more than approximately 40 milliwatts of power, with D. C. inputs of up to 5 Watts. It is clear from these results that the mounting techniques used, while improving the thermal resistance, cause a degradation of oscillator performance. Several possible causes of this disappointing performance are being investigated, including a possible shielding of the junction by a metallic protrusion formed during the mounting.

Using improved conventionally-mounted diodes, however, over 1 watt of peak pulse power was obtained at 8.6 GHz with 7 percent efficiency. This indicates that a sound junction design has been developed, and that thermal limitations must be overcome in order to achieve high CW power levels. The present technique of inverted mounting must be improved so as to permit high average power dissipation without sacrificing device performance. The devices used had junction diameters of about 5 mils, and operated at peak current densities of approximately 1600 amperes/cm^2 for maximum output.

A method of infrared classification of diamonds was developed which permits the identification of class IIa diamonds from other types. Class IIa are nearly nitrogen-free and have the highest thermal conductivity. Of 15 samples measured, 2 were of class IIa and 2 others were nearly low enough in nitrogen content to be so classified.

Further work was done on investigating noise characteristics in avalanche diodes. AM noise spectra measurements were made at frequencies up to 1 GHz off the carrier, and showed that noise output is essentially constant from 200 Hz, which was the lowest frequency measured, up to about 100 MHz, and then decreases at 6 db per octave.

II. DIODE DEVELOPMENT

Work during this quarter has been directed toward improved efficiency of the avalanche diode structure in order that higher powers may be achieved. Activities may be divided into five main efforts:

1. Control of starting material

2. Development of optimized diffusion profile

3. Improved mounting of the diode.

4. Exploration of other means of junction formation.

5. Control of surface properties.

II. 1 Material Studies

Control of the properties of the silicon epitaxial wafers is essential to the evaluation of other processing variables and to obtaining uniformly-controlled avalanche breakdown. To this end, difficulties fall into two categories:

A. Material perfection

As is well known, the uniformity of breakdown is dependent upon the structural perfection of the silicon. Dislocations and stacking faults in the epitaxial layer can contribute to non-uniform breakdown by causing a localized high field (micro-plasma) and by causing diffusion spikes which also create a localized high field. Both of these mechanisms induce non-uniformities in both the plane of the junction and in the direction normal to the junction. These nonuniformities in turn can give rise to high localized currents and to incoherent oscillations (noise).

During this reporting period, material from a number of different sources has been obtained for evaluation. Because of delays in delivery, this material has not been fully processed, so that the evaluation is not complete. Some of the results will be given in this report.

Material of ⟨100⟩ orientation is being compared with ⟨111⟩. Since the direction of the dislocation in ⟨100⟩ material is parallel to the plane of the junction, diffusion spikes should not intersect the junction.

B. Doping Unformity in the Epitaxial Layer

Because of the difficulty in measuring the doping level in epitaxial layers, capacitance - voltage analysis of the epitaxial layer is being performed.

A computer program has been written to permit rapid calculation of the doping profile in the epitaxial layer, and to evaluate the slope of the diffusion front. Some of the results are reported here.

II. 2 Optimization of Diode Structure

Run TP-5 has resulted to the best yield of low noise, high power diodes to date. A series of wafers was therefore processed under identical conditions in order to duplicate these results. Table I lists the initial conditions.

TABLE I

Initial Conditions of Devices Similar to Run TP-5

Device No.	ℓ (μ M)	V_B (Volts)	R_{P_1} (Ω/square)	Deposition Conditions	R_{P_2} (Ω/square)	Diffusion Conditions
TP-5	8.8 - 10.9	70	4	950°C-18 min	13	N_2, O_2 1100°C-60 min
TPP-1	7.2 - 10.2	65-70	4.2	1025°C-20 min	18.6	Wet O_2 1100°C-60 min
TPP-2	8.4 - 10.5	60-70	3.6	1025°C-20 min	5.7	Dry O_2 1150°C-40 min
24-499-62	9.75	60	4.3	1025°C-20 min	7.7	Dry O_2 1150°C-70 min
24-500-20	10.8	65	4.1	1025°C-20 min	8.0	Dry O_2 1150°C-70 min
24-523-37	10.8	57	4.2	1025°C-20 min	8.0	Dry O_2 1150°C-70 min

where ℓ = thickness of epitaxial layer
V_B = breakdown voltage of three point probe measurement
R_{P_1} = sheet resistance after boron deposition
R_{P_2} = sheet resistance after boron diffusion

Table II gives the results of these experiments compared to TP-5.

TABLE II

Oscillator Test Results

Exp.	V_{in}	I_{in}	P_{in}	P_{out} (CW)	% Eff.
TP-5	90-100V	25-30mA	2.5-3.0W	50-150mw	up to 5%
Repeat of TP-5					
TPP-1	80-90V	25mA	2.0-2.25W	20-30mw	1.3
TPP-2A	80-90V	25mA	1.8-2.2W	10-40mw	1.8
TPP-2B	75-80V	30-40mA	2.25-3.2W	35-105mw	3.3
24-499-62	60-70V	25mA	1.5-1.75W	3-6mw	0.34
24-500-20	105-120V	25mA	2.62-3.0W	40-50mw	1.65
24-523-37	80V	25mA	2.0W	4-10mw	0.5

Diodes of group 24-500-20 have been tested with a pulsed input, and outputs of 1 W have been obtained. This suggests that the diode's output under CW conditions is limited only by the thermal limitations of the structure.

As can be seen, there is considerable variation in the results obtained, with no particular correlation with process conditions. One result that should be noted is that the 24-499, 24-500 and 24-523 groups exhibited somewhat lower noise performance than the TPP groups. These groups represent different material sources and may very well reflect differences in material perfection.

II. 2. 1 Study of Different Impurity Distributions

Three structures were selected for investigation:

A. Retrograde $P^+N\nu N^+$

A retrograde doping profile was evaluated because the resulting field distribution would localize the avalanching region near the junction. This in turn should result in a lower threshold for oscillation and higher efficiencies.

The structure obtained would represent a hyper-abrupt junction rather than a Read Structure.

The retrograde material has characteristics as shown in Figure 1.

A guassian "P" diffusion 1μM deep resulted in devices with a rather soft V_B (25-45V at 10μA) and a second distinct breakdown region at 60V (1mA). Subsequent "etching in the package" resulted in several units with V_B of 50-60V at 10μA. However, a C-V plot of these diodes showed essentially square law dependence with no hyper-abrupt or punch-through characteristic prior to breakdown. This, coupled with the abnormally high Rs (reflectometer) readings observed, seems to indicate that the high resistivity N region has not been reached or included in the depletion layer. As to be expected, these units also showed no oscillation. A section has been bevelled and stained in an effort to account for the present results prior to proceeding with additional runs.

B. $P^+\nu N^+$

The results of the $P^+\nu N^+$ test runs were essentially the same as those for the retrograde, excluding the double breakdown. V_B's after diffusion were 70-90 Volts but with no punch-through. The initial results of both tests seem to indicate too shallow a diffusion, and a bevel and stain is being processed to confirm this.

C. P^+NN^+

The P^+NN^+ test had as its goal the reproduction of a previous run (TP-5) which made use of 7-10μM epi with 3 μM diffusion. However, the available material was either shallower (5-6μM) or much thicker (9 - 13 μM). Although initially a 10-11 μM layer on As was selected, it was dropped during processing for the 5-6 μM range which is available both on <111> and <100> Sb-doped substrates. Both a modified gaussian and erfc diffusion of ~1μM depth have been processed, and subsequent bevel and stain of sections of the slice have indicated that the desired profiles have been attained as indicated in Figure 2.

No results are as yet available on finished units.

II. 3 IMPROVED DIODE MOUNTING FOR BETTER HEAT DISSIPATION

Two parallel efforts are being pursued in order to arrive at an optimum mounting technique. Conventional mounting techniques (junction side up) are being studied in order to determine the best bonding and interface materials and processes to reduce diode-to-mount thermal resistance.

FIGURE 1
DOPING PROFILE RETROGRADE EPITAXIAL LAYER

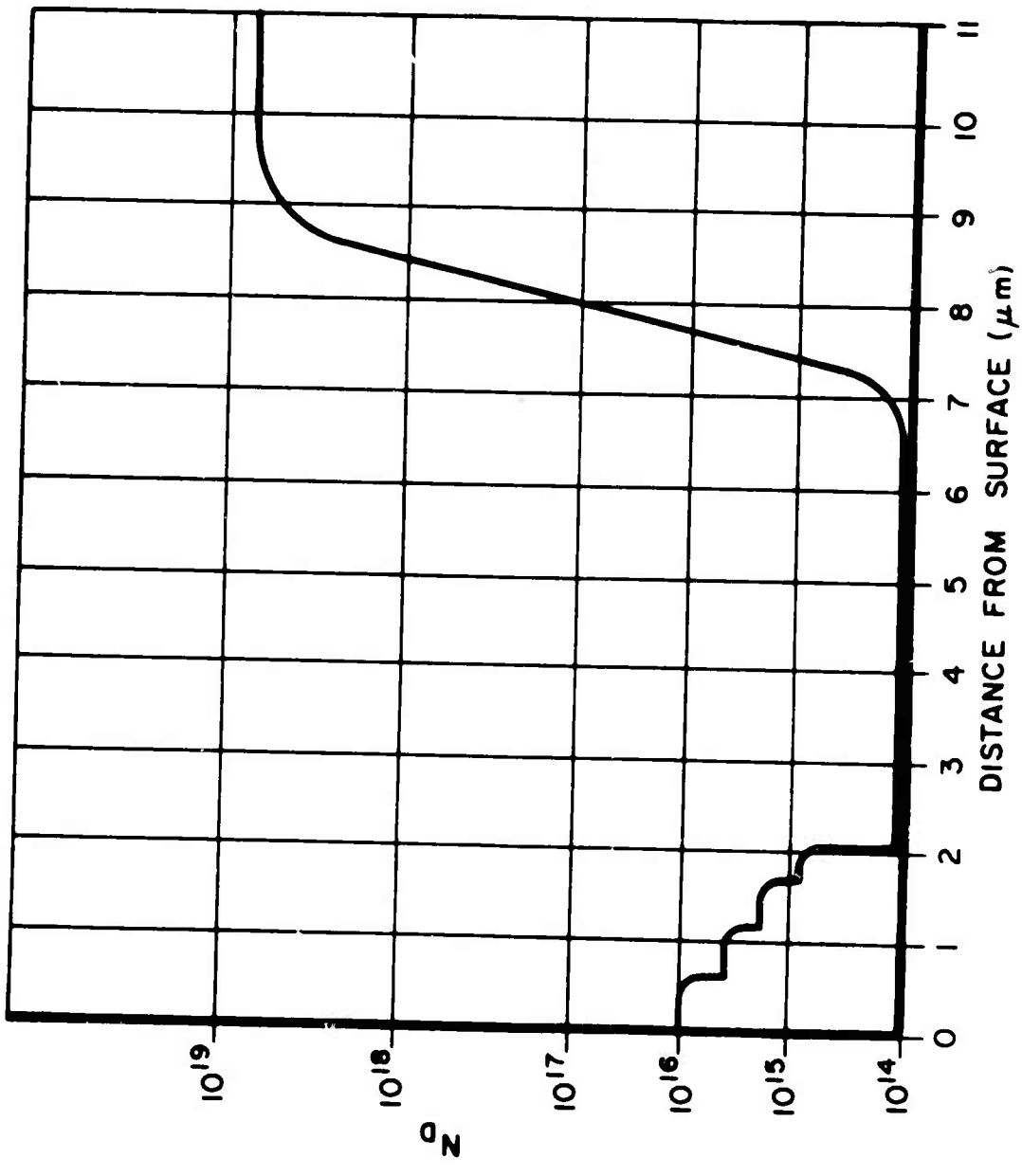

FIGURE 2
DOUBLE DIFFUSION DOPING PROFILE

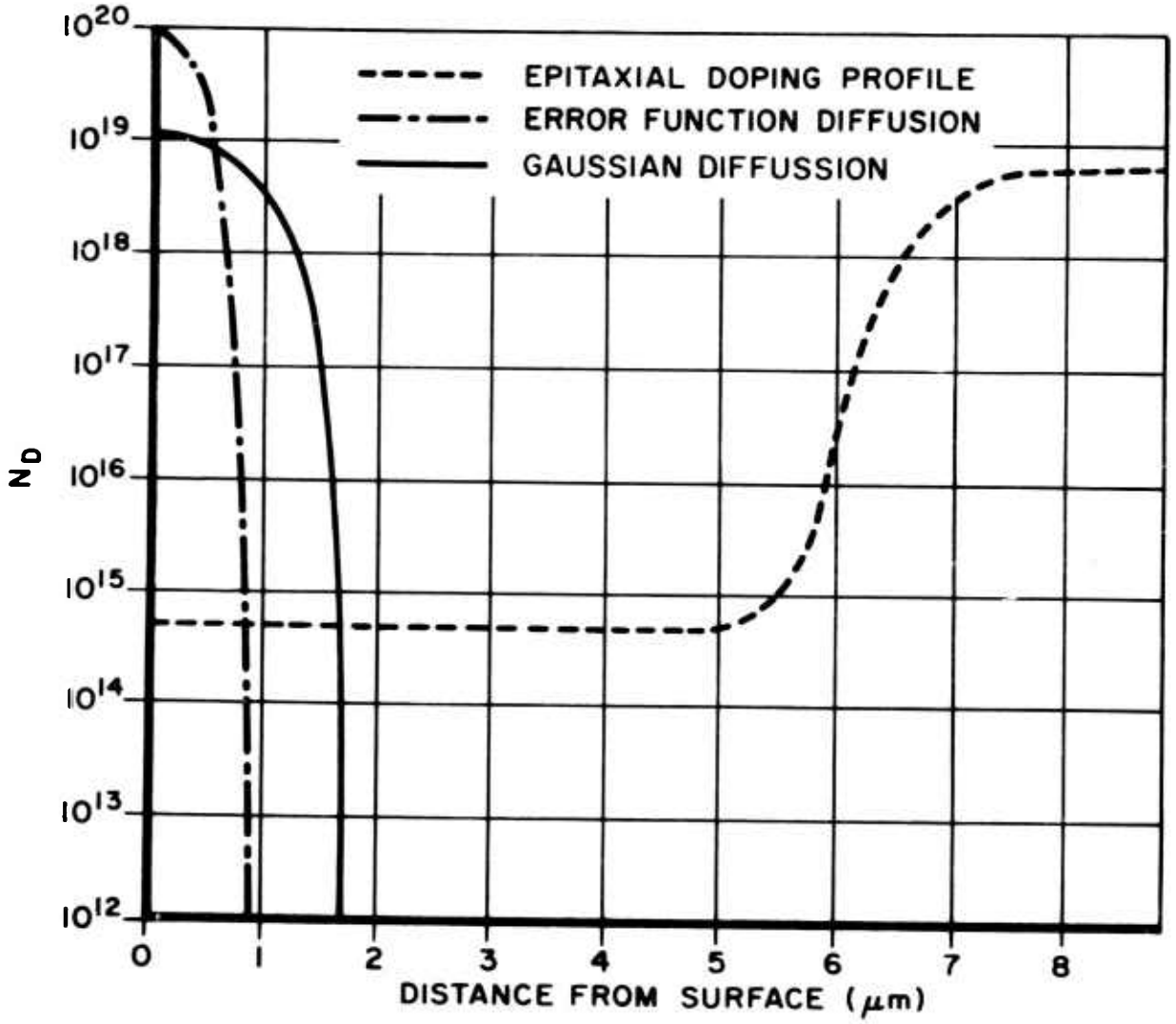

Inverted chip (junction side down) mounting techniques are being developed to maximize heat transfer from the junction to the heat sink so as to permit dissipation of up to 20 Watts D.C. power per chip in the final device configuration.

II. 3. 1 Conventional Mounting

In order to reduce the thermal resistance in the avalanche oscillator diode, and to narrow the spread of R_T values presently obtained, an intensive investigation of the problem has been initiated. The approach is as follows:

A matrix of experimental procedures will be followed in which the experimental variables are

(1) the mounting technique

(2) the pin material

TABLE III

Mounting Experiments

Pin Material	Eutectic	Thermocompression	Ultrasonic
Cu-Mo-Au	x	x	x
Cu-Ni-Au	x	x	x
Cu-Ag-Au	x	x	x

To insure validity of results, diode chips from a single slice were used. The metallization of the back of the slice was consistent with the requirements of all methods.

Evaluation of the mounted dice is being made as follows:

1. R_T measurements
2. Metallographic analysis
3. Electron beam microprobe analysis
4. Environmental analysis

The initial results show the Cu-Ag-Au pin structure to be significantly superior both in electrical and thermal resistance to both of the other two structures, with the eutectic mounting technique. The other two methods will be studied in the next quarter.

Table IV shows the preliminary data.

TABLE IV

Thermal Resistance Data

Pin Structure	Average I_F at 1V	Average Thermal Resistance
Cu-Mo-Au	9.7 mA	33°C/W
Cu-Ni-Au	57 mA	28°C/W
Cu-Ag-Au	120 mA	26°C/W

II. 3. 2 Inverted Chip Mounting

Development of inverted mount diodes is proceeding by mounting diodes on copper heat sinks, and mounting diodes on diamonds embedded in copper heat sinks. The discussion which follows concerns inverted mounting on copper; the junction formation and bonding will be quite similar on diamond.

Five wafers were processed to produce inverted chips. There were some problems in the back side etching. The diffusion conditions were as follows:

TABLE V

Diffusion Conditions For Inverted Mounting Diodes

Device No.	ℓ (μM)	V_B	R_{P_1} (Ω)	Deposition Conditions	R_{P_1} (Ω)	Diffusion Conditions
TP-49	8.5-9.5	85V	14.8	950°C-18 min.	15.7	1100°C-65 min.
TPP-5	7.8-8.2	65V	14.8	950°C-18 min.	15.7	1100°C-65 min.
SM-49801-15	5.8-6.4	60-70V	14.8	950°C-18 min.	15.7	1100°C-65 min.
SM-49801-17	6.2-6.7	68-72V	14.8	950°C-18 min.	15.7	1100°C-65 min.
100-212	6.25 μ	55-65V	14.3	950°C-18 min.	3.0	1100°C-65 min.

where the quantities in the headings are as defined in Table I.

The chips were mounted anode side down and tested. The results were:

TABLE VI

Results of Tests On Inverted Mount Diodes

Device No.	V_{in}	I_{in}	P_{out}
TP-49	82 - 96V	40mA	10 - 30 mw
SM-49801-15	70 - 80V	50mA	2 - 8 mw
SM-49801-17	80 - 100 V	30 - 50 mA	15 - 40 mw
100-2-2	80 - 95V	40 - 50 mA	10 - 40 mw

The results are quite disappointing in that the efficiency in this configuration is significantly lower than expected. Note that these devices operate at higher input power levels than do the conventionally mounted units. Thermally, these appear to be better devices, having measured thermal resistance values of 20-30°C per watt, as compared to 30-40°C per watt for conventionally mounted devices, but efficency is low. It has been postulated that protrusions of the bonding metal near the diode junction may be interfering with the radiation of output power. This question is being investigated further.

II. 3. 3 Properties of Diamond as a Thermal Heat Sink Material

It has been established that diamond IIa is thermally more conductive than copper at room temperature and hence is attractive for use in the design of the heat sink, as described in the First Quarterly Report. The relative availability and the differences in the various types of diamond are of concern and will be treated here. The two principle classes of diamond are type I, which contains a large amount of nitrogen as an impurity, and type II, which has a relatively small amount of nitrogen. Diamond Ia is a sub-class which contains precipitates of elementry nitrogen which crystallize in platelet form. The platelets can be observed with an electron microscope and have maximum dimensions extending from 100 to 1000 Å. In this type of diamond the nitrogen content extends from 0.05 to 0.25%. Diamond Ib differs from diamond Ia in that it contains nitrogen in dispersed rather than in precipitate form. A portion of the nitrogen may possibly appear in substitutional form in the crystal lattice, but this is not firmly established. Diamond II, as mentioned earlier, contains a relatively small amount of nitrogen which, at most, is 10 parts

per million. Type IIa and IIb differ in that the latter contains small traces of other impurities which makes it semiconducting, whereas the former is an insulator. From the above discussion, it should not be concluded that all diamond can be clearly typed in a class or sub-class. Intermediate types of diamond frequently occur in nature, implying "in-between" amounts of nitrogen. In addition, one diamond crystal may often be so inhomogeneous, that several types of diamond occur in the sample.

From a theoretical point of view, it is to be expected that the highest thermal conductivity should be obtained for the most perfect crystalline form of pure diamond. From the above description, it would be expected that type IIa diamond, which is the purest form diamond, would most likely yield the highest thermal conductivities, providing the crystalline structure differs little from the ideal. It is possible that one could obtain samples of type IIa which are not highly thermally conductive because of crystalline imperfections. Direct measurements of the thermal conductivity of diamond are, in fact, the only way to ensure high conductivities. However, such measurements are difficult and expensive to carry out in that they require relatively large samples cut to proper test shapes. There have been a very limited number of thermal conductivity measurements on diamond and the results are summarized in "Physical Properties of Diamond," edited by R. Berman, Clarendon Press, Oxford, 1965. From the small number of samples measured, it appears that diamond IIa yields the higher thermal conductivities. However, it is entirely possible that with more extensive conductivity measurements, one could find high thermal conductivities in certain select samples of type Ib diamond.

For the purposes of the contract, the only practical source of diamond is natural stones, since synthetic diamond is too small in size as presently manufactured. The most abundant form of natural diamond is type I. It is estimated that 30% of natural diamond is type II, but since single samples are most often inhomogeneous, the location of a single crystal of type IIa diamond might be somewhat more rare than indicated by the 30% figure.

The various types of diamond can be determined by their infrared absorption spectra. Figures 3 and 4 illustrate the differences in the spectra of type Ib and IIa. In order to make such measurements, the samples have to be shaped to have two optically polished parallel surfaces. A number of measurements were made on various samples of diamond and the results will be reported later in a section of Infrared Spectra Measurements on Diamonds.

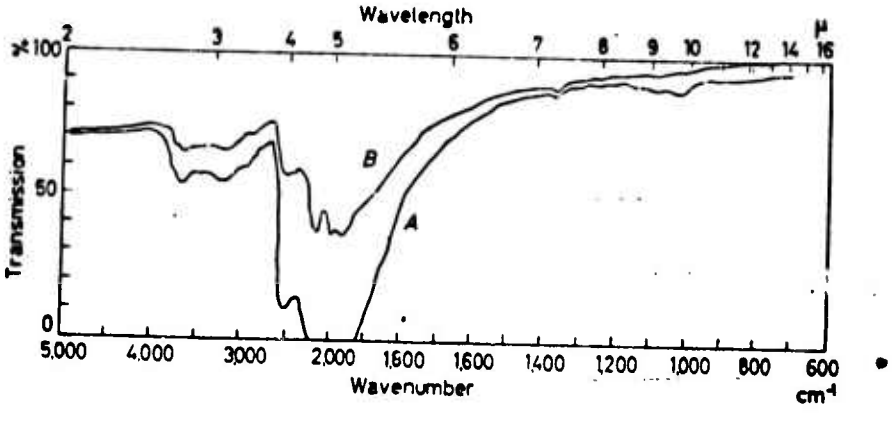

FIGURE 3

A. Infra-red spectrum of a typical type II diamond (2.4 mm thick)

B. Infra-red spectrum of a thin type II diamond (1 mm thick)

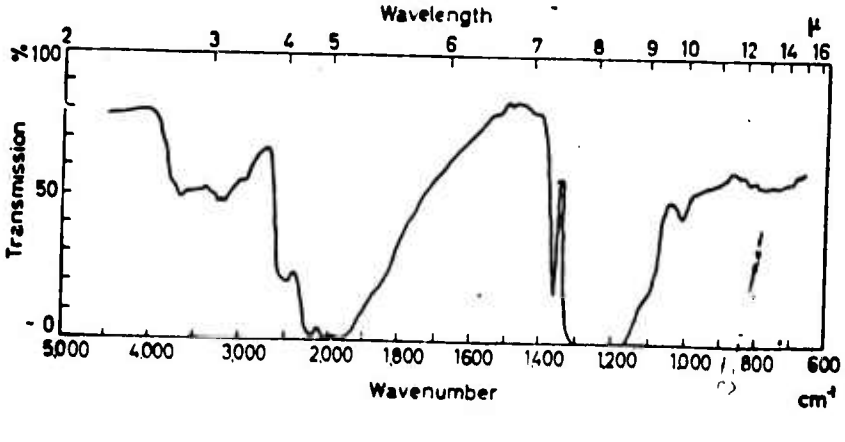

FIGURE 4

Infra-red spectrum of a typical type I diamond (2.4 mm thick)

II. 3. 4 Method for the Measurement of the Thermal Conductivity of Irregularly Shaped Diamonds Having One Plane Surface

This section suggests a method for the measurement of the thermal conductivity of irregularly shapped homogeneous materials having one planar surface. The measurement method was conceived for the purpose of determining the thermal conductivity of diamond but is applicable for measuring other materials. Consider a diamond sample which has at least one flat surface as represented in cross-section in Figure 5. The diamond sample is surrounded by a heat bath of a homogeneous substance such as oil (a metal heat bath is also possible) contained in a heat insulating glass Dewar. The surface of the heat bath is flush with the flat surface of the diamond as shown. The bath is heated by a resistive element with an electrical power imput, P_e. The temperature of the heat bath is measured by a thermometer, which is observed through a non-silvered part of the glass wall of the Dewar. This temperature is assumed to be uniform. The latter condition can be assured by using a mechanical stirrer in the case of a liquid bath. In steady state, the total electric input P_e is converted to heat power, P_h, which is conducted through a diamond to the pointed thermocouple. The thermocouple serves the dual purpose of (1) providing a means for temperature measurement at the point contact and, (2) providing a heat path to the outside environment. Thus in steady state,

$$P_e = P_h, \tag{1}$$

and the temperature of the point contact and the heat bath are T_c and T_b, respectively. It has been shown[1] that, for a perfectly hemispherical material of heat conductivity, χ, which is contacted by an isothermal hemispherical contact and placed in an isothermal heat bath as indicated in Figure 6, the following holds

$$T_2 - T_1 = \frac{P}{2\pi\chi}\left[\frac{1}{r_1} - \frac{1}{r_2}\right] \tag{2}$$

where P is the total heat power flow from the heat bath through the material in question. All other symbols are defined in the figure. If $r_2 \gg r_1$, then

$$T_2 - T_1 \cong \frac{P}{2\pi\chi r_2} \quad ; \tag{3}$$

inverting,

$$\chi \cong \frac{P_e}{2\pi(T_2 - T_1)r_2}. \tag{4}$$

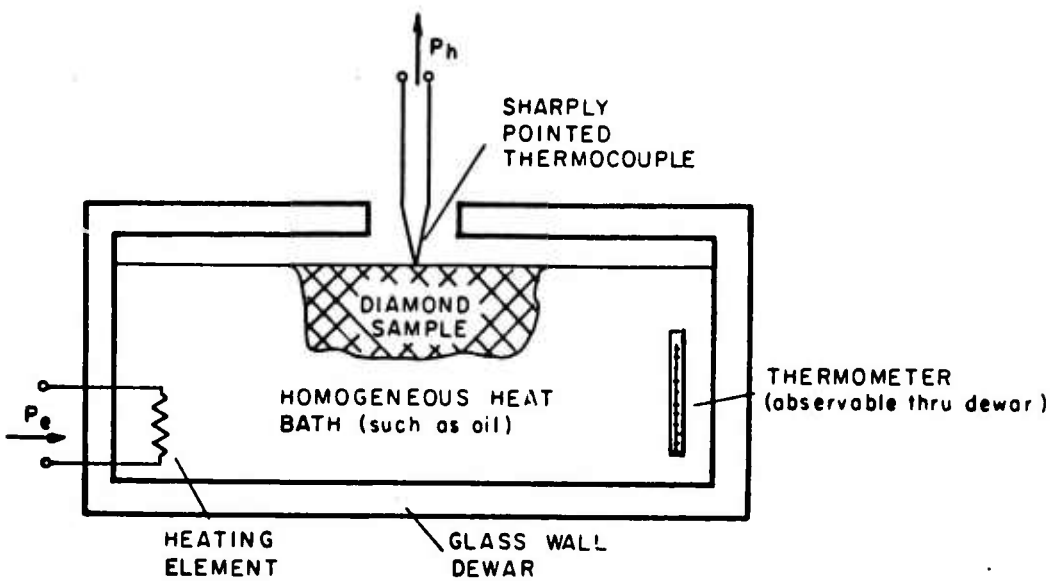

FIGURE 5

Diamond Sample Mounted In Heating Bath

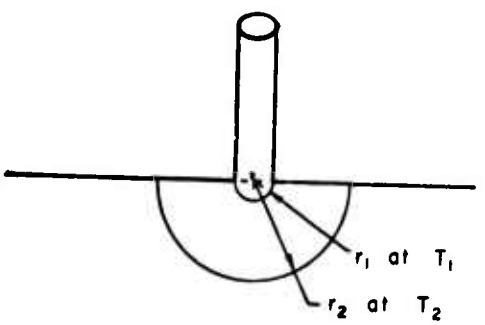

FIGURE 6

Hemispherical Material With Isothermal Contact In Isothermal Heat Bath

This formula is applicable to the structure shown in Figure 5, provided the radius of the point contact is known and the minimum radical distance from the contact to the outer irregular surface of the diamond is comparatively large. It then follows

$$\text{Heat Conductivity of diamond} = \chi = \frac{P_e}{2\pi(T_b - T_c)r_c} \tag{5}$$

where r_c is the radius of the point contact. If r_c is not known, it is still possible to use this method for the determination of the relative heat conductivities of diamond and other structures. It should also be noted that the electrical heat source could be placed on the point contact thermal structure and flow of heat reversed. In this case, the formulas and the methods presented are still valid.

II. 3. 5 Infrared Spectra Measurements on Diamonds

A number of diamond specimens were obtained on consignment for purposes of classification such that diamond IIa samples could be sorted out and purchased. The samples were prepared, for test purposes, with two flat parallel surfaces separated by about 1 mm. Figures 7 through 12 illustrate the spectra obtained on 15 separate samples. Comparison with Figure 3 and Figure 4 indicates that at least two samples are type IIa, and one or two other samples are close to this classification.

II. 4 Exploration of Other Methods of Junction Formation

Because diffused junctions are invariably graded to some extent, and also subject to diffusion spikes, alternate methods of junction formation were explored. These were ion implantation and Schottky barrier formation.

II. 4. 1 Ion Implantation

Three wafers were ion implanted and evaluated as avalanche oscillator diodes. Two of the three had boron diffused to a depth of 1 μ M in order to reduce the series resistance of the P layer. The third wafer had no previous diffusion.

Ion implantation produces a Bragg distribution of implanted particles. Therefore, the P-N junction produced is very abrupt.

The undiffused wafer produced no oscillation due to low breakdown. Of the two diffused wafers, the first showed surface instability due in part to excessively high breakdown voltage ($>$ 120 Volts). On pulse test, however, oscillation with 180-200 milliwatts output was observed.

FIGURE 7

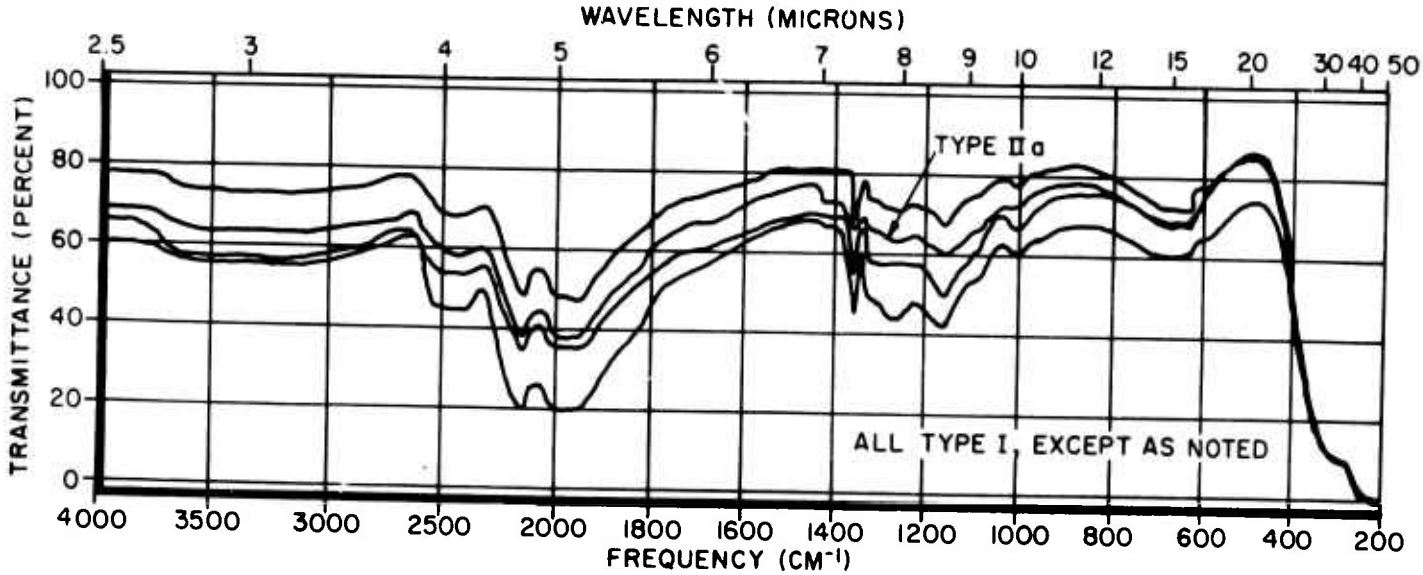

FIGURE 8

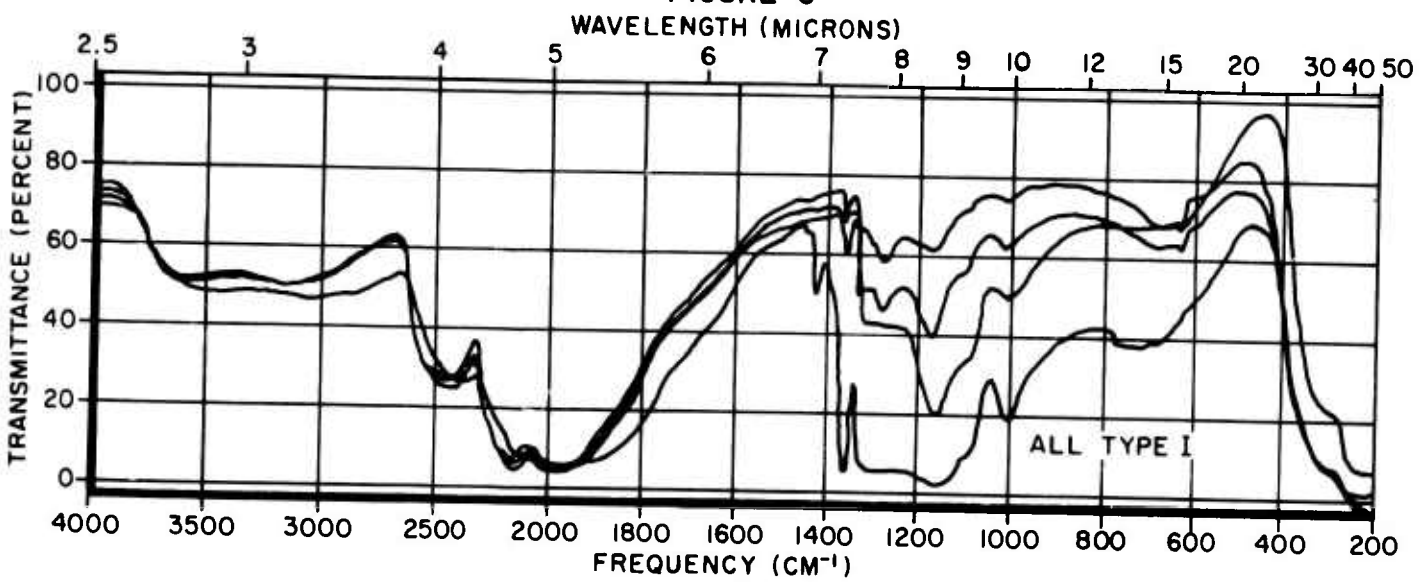

INFRARED SPECTROGRAPHS OF DIAMOND SAMPLES

FIGURE 9

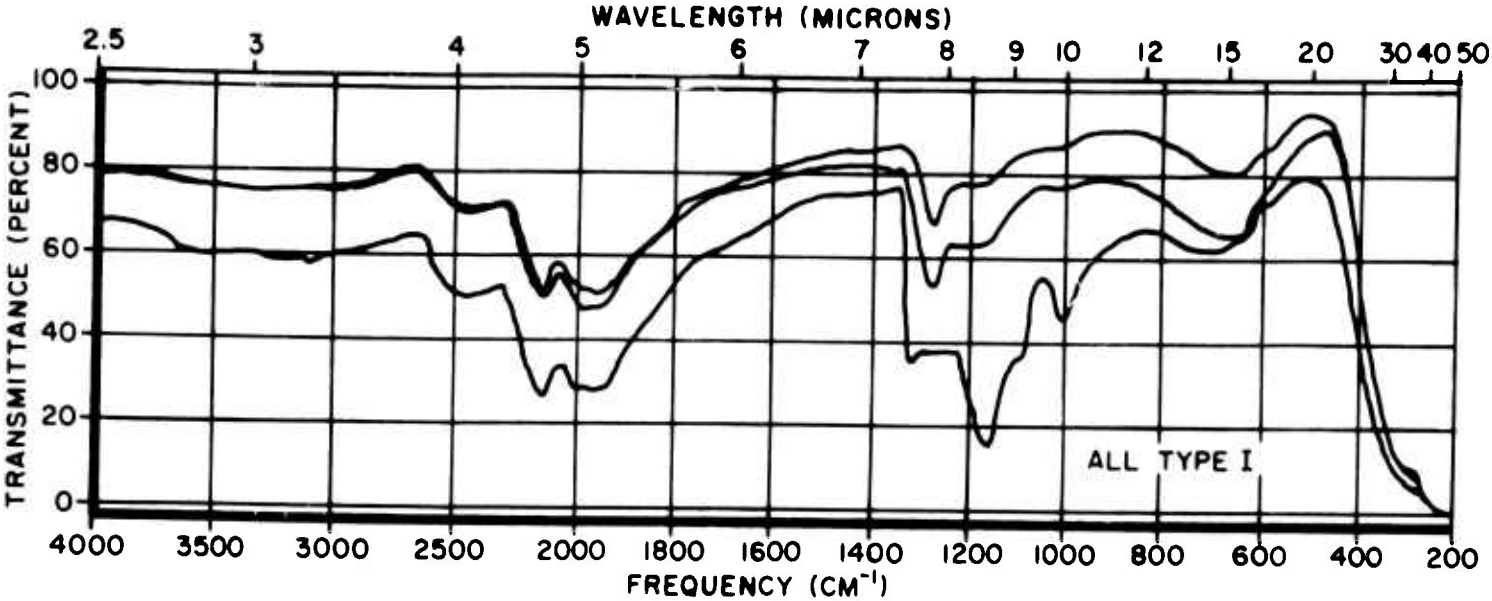

FIGURE 10

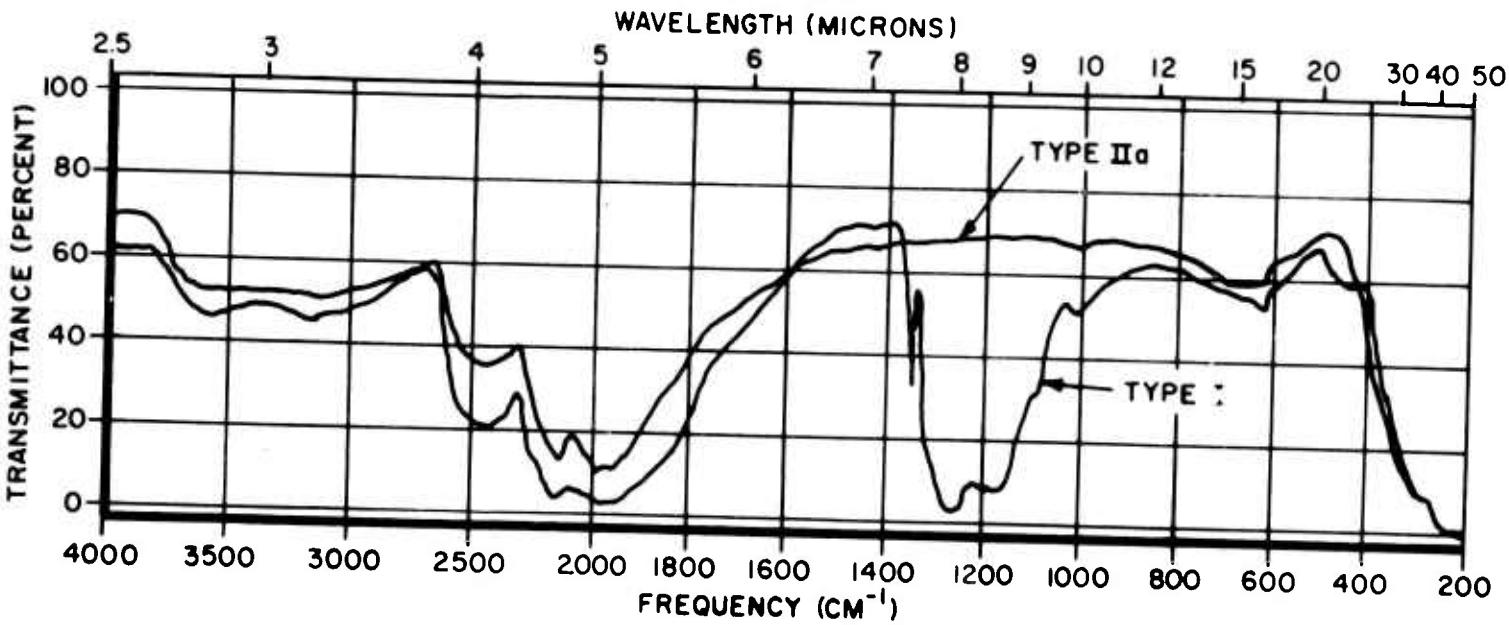

INFRARED SPECTROGRAPHS OF DIAMOND SAMPLES

FIGURE 11

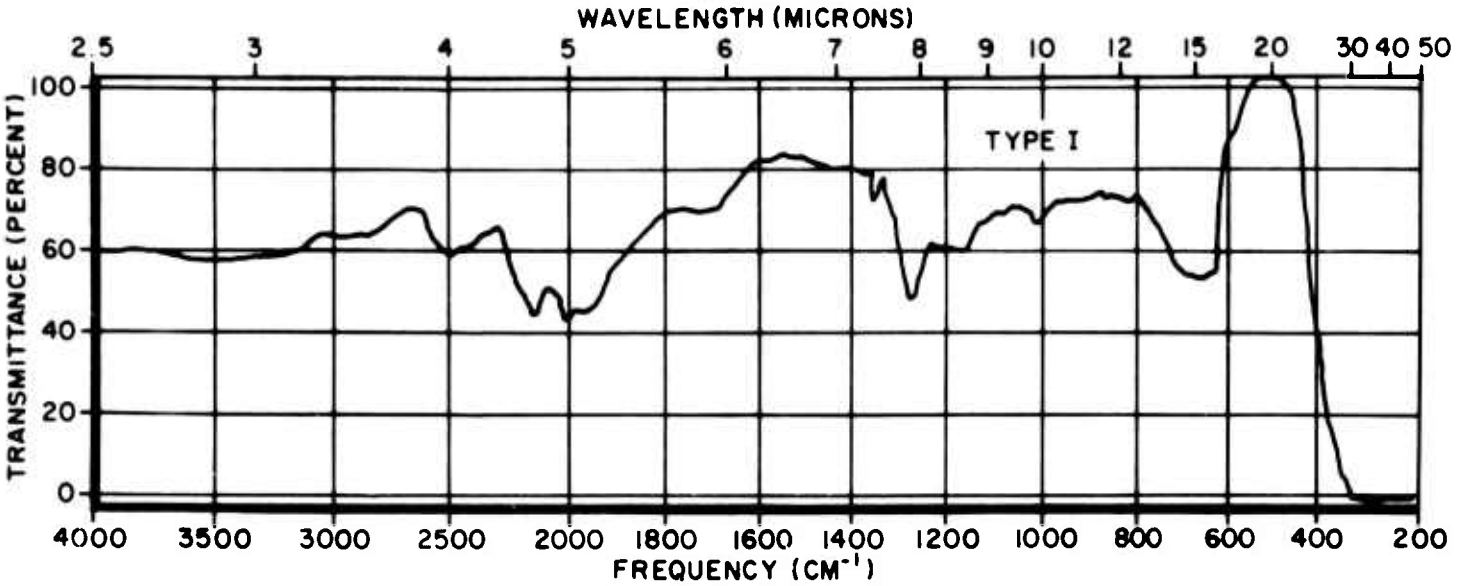

FIGURE 12

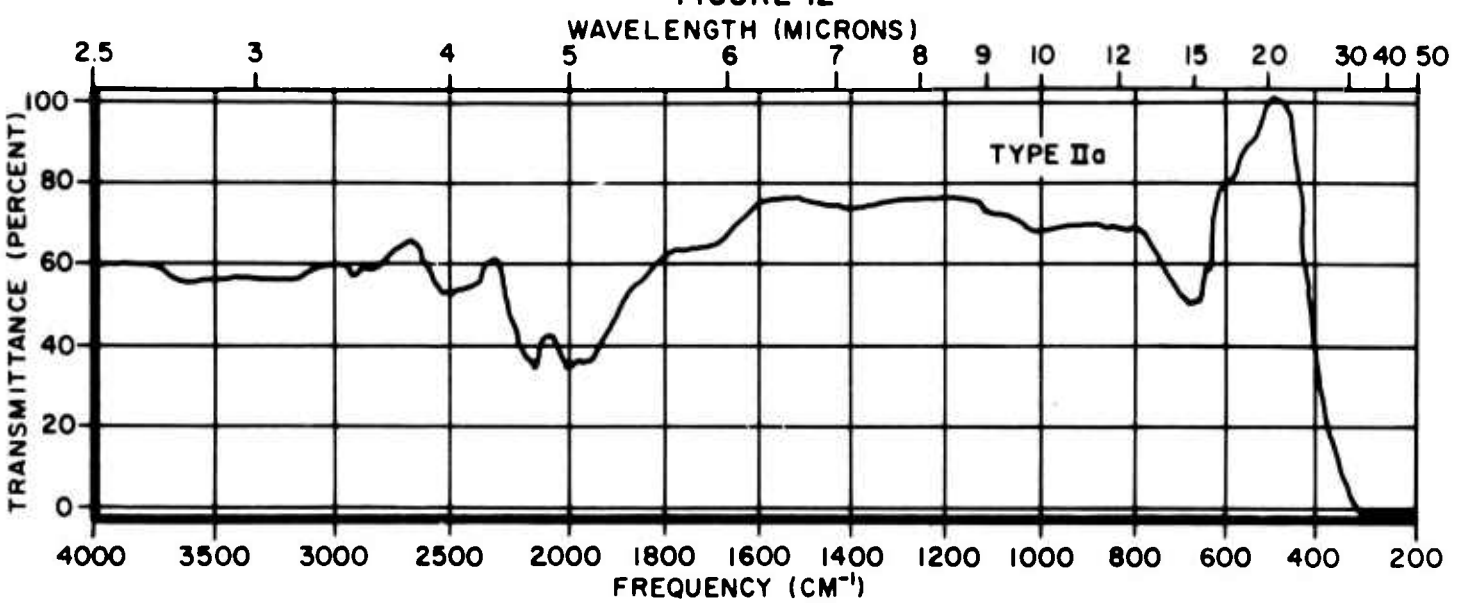

INFRARED SPECTROGRAPHS OF DIAMOND SAMPLES

The second wafer punched through before breakdown with little power output being observed. One diode, however, did not punch through and gave 25 milliwatts output. This approach will be further explored.

II. 4. 2 Schottky Barrier Avalanche Diode

In order to evaluate a structure in which the field distribution could be considered to depart from linearity only as a function of doping irregularities in the epitaxial layer, two slices were processed as Schottky barrier diodes. The resulting units oscillated, giving 20-25 mw output, but the efficiency was low (<1%) and the output was very noisy. The noise is felt to be due to variations in the fringing fields at the edges of the junctions.

Consideration is being given to a guard ring structure, so that the bulk effects can be better observed.

II. 4. 3 Gold Doping

Since the avalanche process depends on the generation of carriers in the high field region, it can be seen that, if the lifetime is sufficiently long the diode can swing out of the avalanche region under high power oscillating conditions, and re-establishment of avalanche can not take place for a time of the same order as the transit time, due to too low a rate of carrier generation. To increase the carrier generation rate, one wafer has been gold doped and processed. Results were not available at the time of writing.

II. 5 Control of Surface Properties

Since the avalanche oscillator diode is required to operate stably in the avalanche region, it is necessary that the surface properties do not determine the breakdown. In order to assure high breakdown and prevent instability due to surface contamination, passivation of the junction is being explored.

The first experiment to this end has been done during this quarter. One half of a wafer was mesa etched and a 600 Å layer of pyrolytic oxide deposited. The other half was packaged by conventional techniques.

D. C. probe data, taken on the oxide coated slice showed reverse breakdown and currents comparable to the packaged diodes from the same slice. Unfortunately, the passivated wafer was lost in the dicing operation due to operator error. The experiment is being repeated. If successfully done, passivation will not only eliminate surface problems as such, but greatly reduce the problems encountered in inverted chip bonding.

In addition to pyrolytic oxide deposition, thermally grown oxides and oxide grown by plasma anodization, as well as complex passivating structures, will be explored.

III PULSED OSCILLATOR CIRCUIT TESTS

Results given in the previous report were on a continuous wave basis. As an indication of junction design optimization, exclusive of heat sinking, it is preferable to measure oscillator performance on a narrow pulse basis to avoid excessive heating of the junction. During this reporting period, a pulse test set-up was assembled. Figure 13 shows a block diagram of the set-up. A pulse generator with a peak power capacity of approximately 40 watts and variable pulse amplitude provides the drive power for the test oscillator. Pulse amplitude and current are measured by a peak voltmeter and a precision inductive current probe, respectively. The RF pulse waveform is monitored with a calibrated crystal detector and displayed simultaneously with the diode current on the scope. In order to improve the detector transient response, the crystal is terminated with a low impedance (50 ohms). The resulting loss of sensitivity is compensated for by a pulse amplifier. Pulse testing has the following advantages:

(a) Electrical and thermal effects can be separated.

(b) The diode can be tested far beyond the thermally-limited cw power level without destruction of the device.

III. 1 Diode Evaluation

Several different junction designs in conventional and inverted chip mounting have been evaluated. All the inverted junction diodes measured to date exhibited electrical saturation effects at input power levels considerably below their thermal limits as seen in Figure 14, which shows data taken under pulsed conditions. Figure 15 shows a similar plot of a newly fabricated run of diodes with conventional mounting of the chip. These diodes are approximately 5 mils in junction diameter. The saturation level here is increased by a factor of about 5 compared to the results obtained with the inverted mount diodes. The diode with conventional mounting is clearly temperature-limited and should produce one watt of cw power when mounted junction side down on an effective (diamond) heat sink, with an efficiency of approximately 7 percent.

Figures 16a and 16b show power output and diode current under pulsed operation for the conventional and inverted mount devices, respectively, described above. These photographs were taken under maximum output conditions for both diodes. That is, further increase in current produced lower output. Figure 16c shows the diode voltage and current waveforms

FIGURE 13
PULSE TEST SET-UP

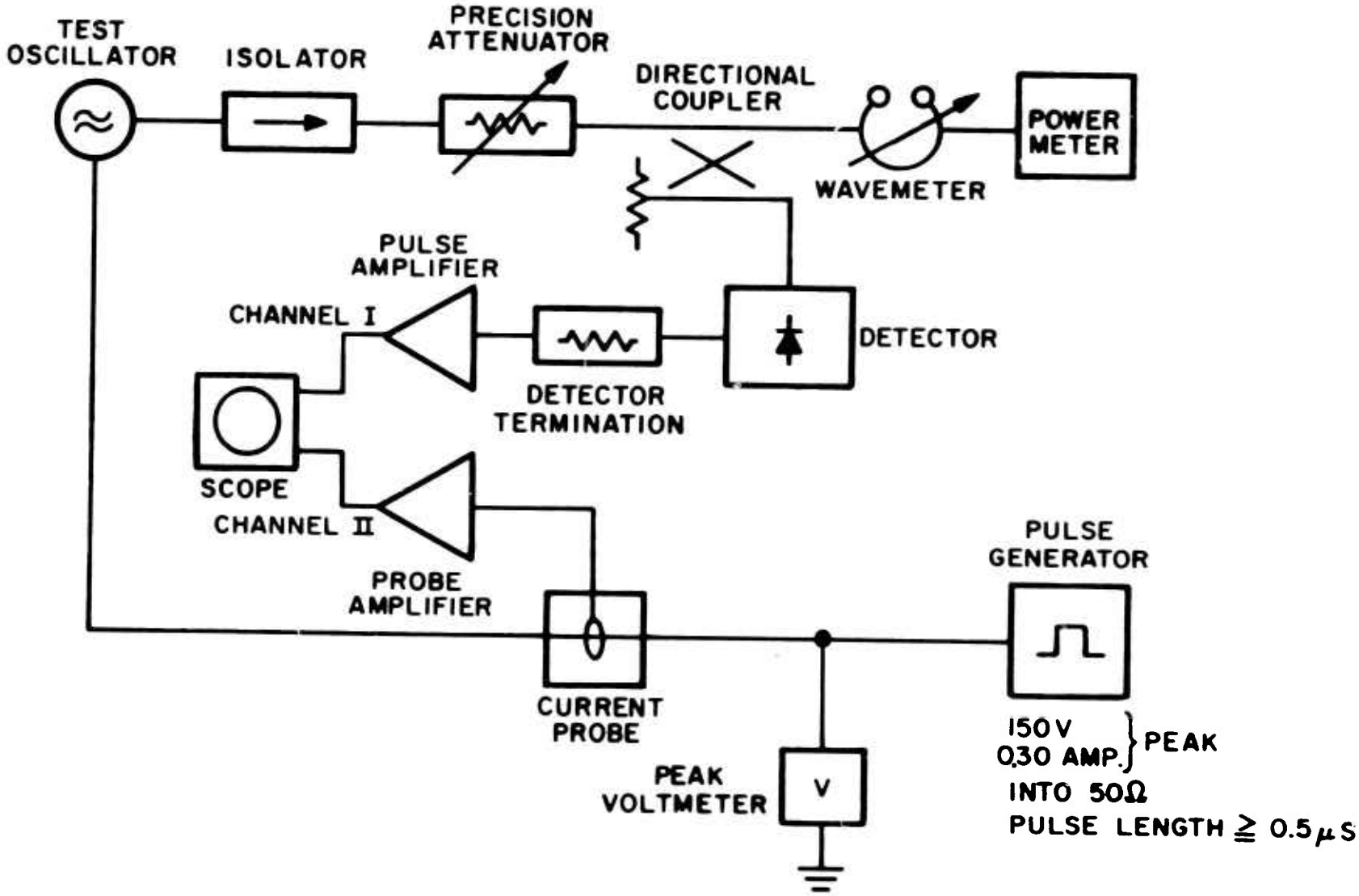

FIGURE 14
PULSED OSCILLATOR OUTPUT AND EFFICIENCY
OF INVERTED MOUNTED DIODE

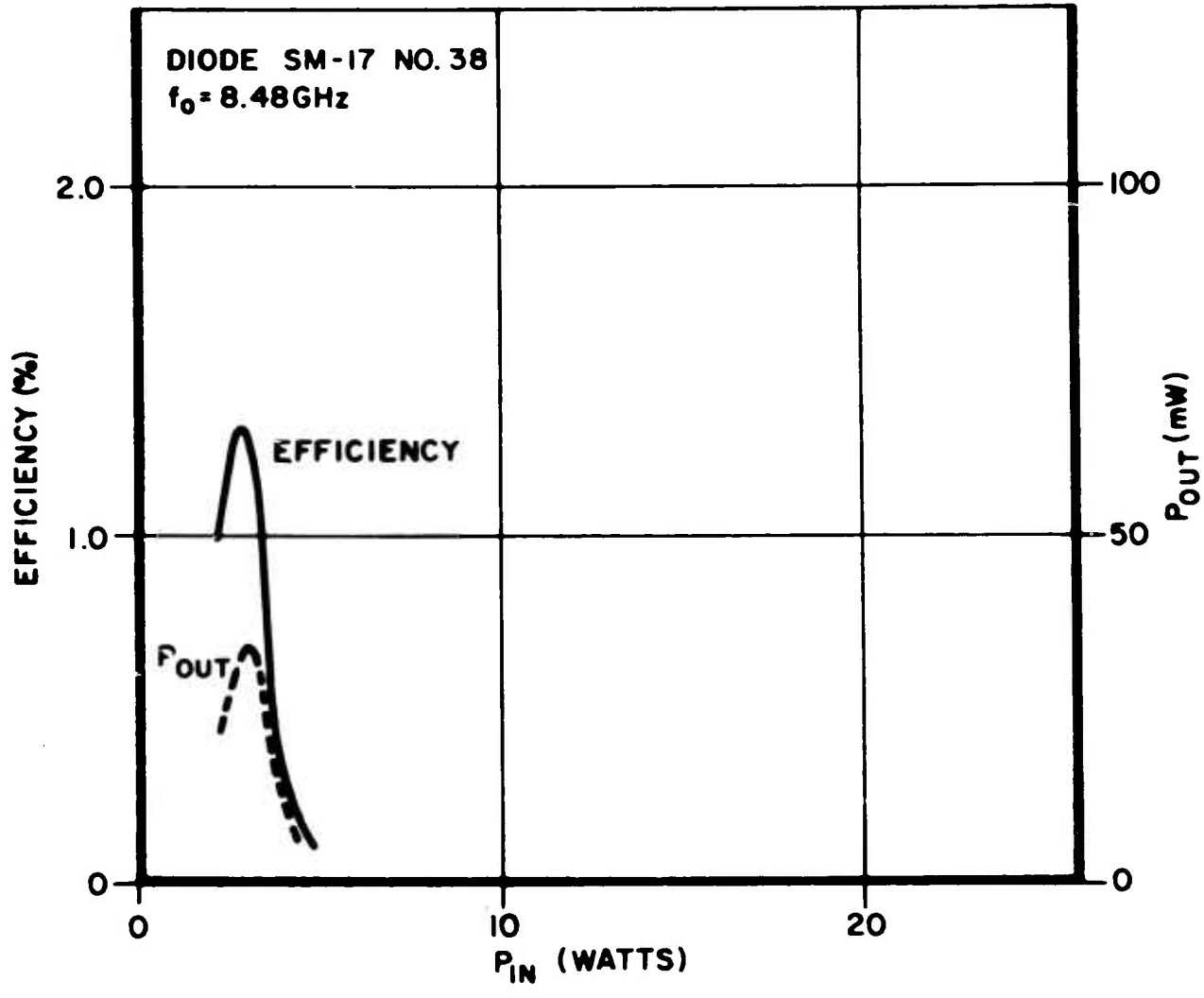

FIGURE 15
PULSED OSCILLATOR OUTPUT AND EFFICIENCY
OF CONVENTIONALLY MOUNTED DIODE

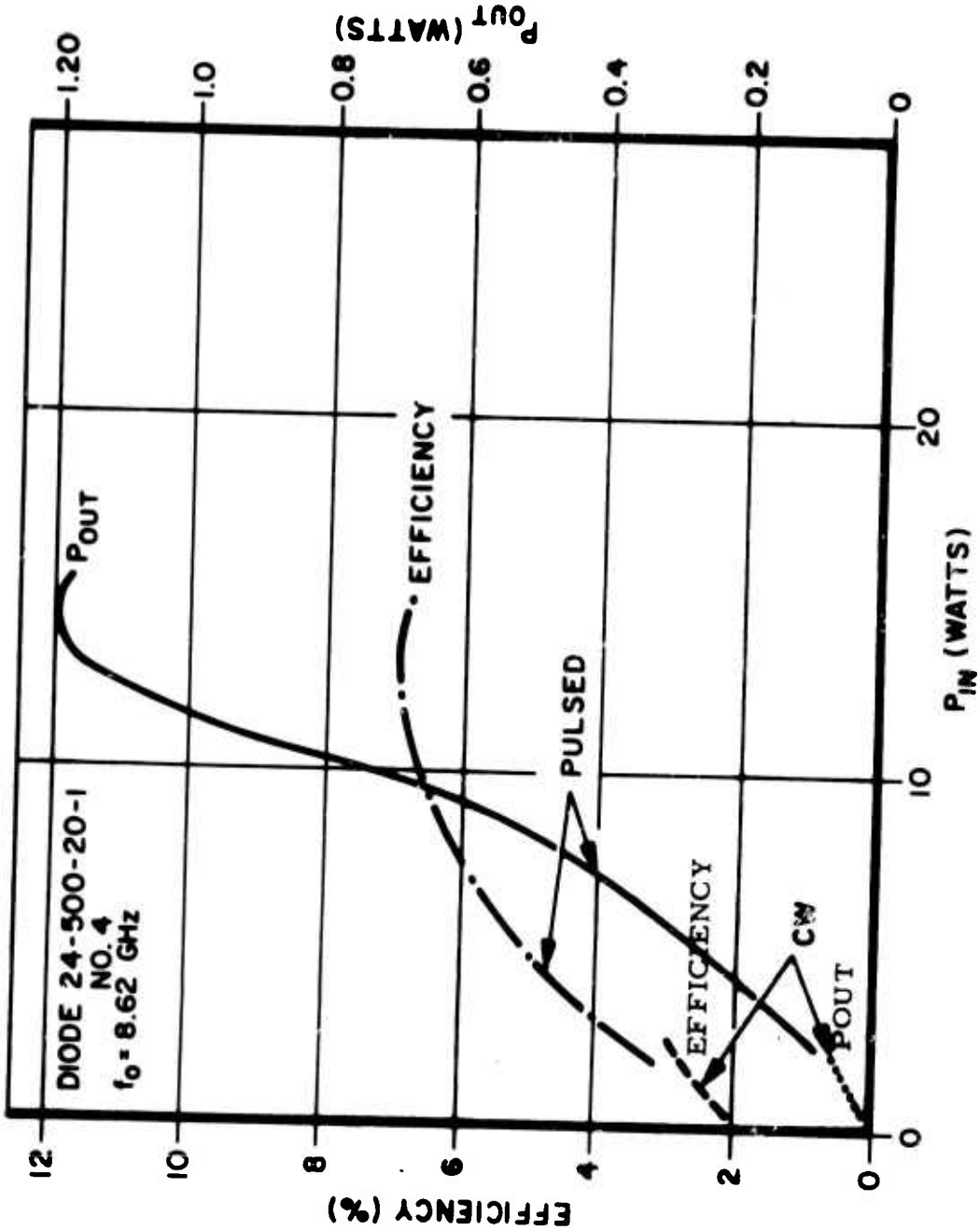

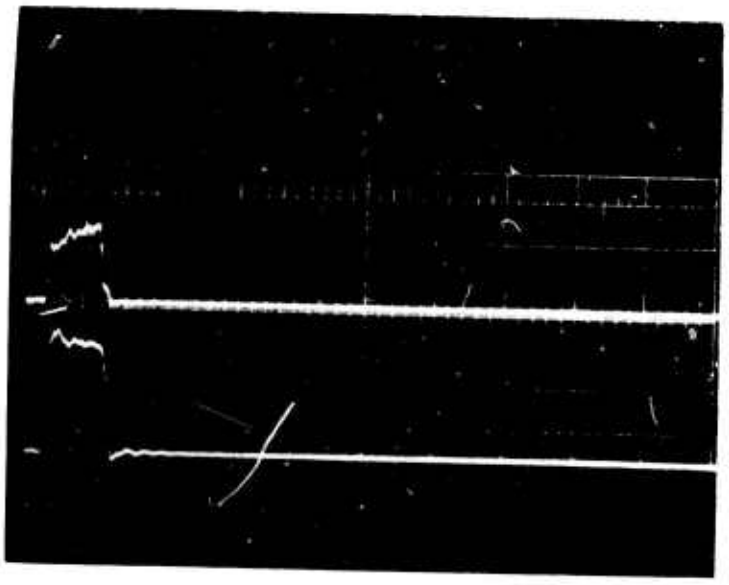

a

Diode 24-500-1 #4 (conventional)

Top: P_{out} = 1 w/division

Bottom: I = 50 mA/division

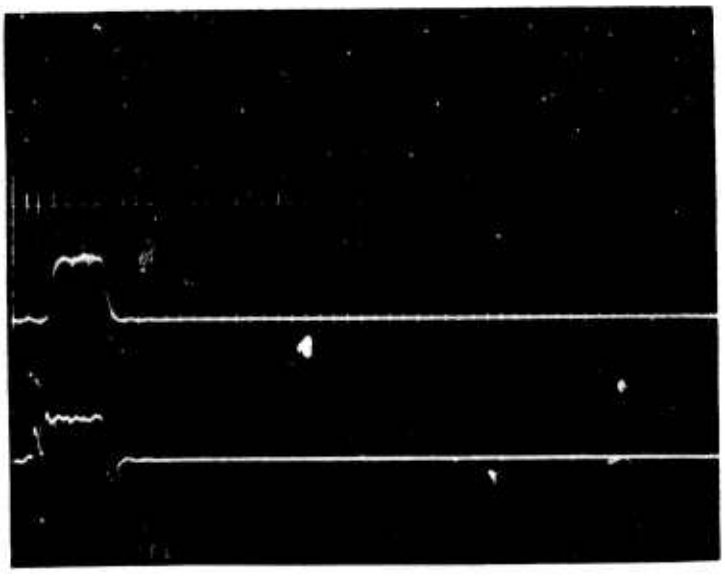

b

Diode SM 17 #8 (inverted)

Top: P_{out} = 50 mw/division

Bottom: I = 50 mA/division

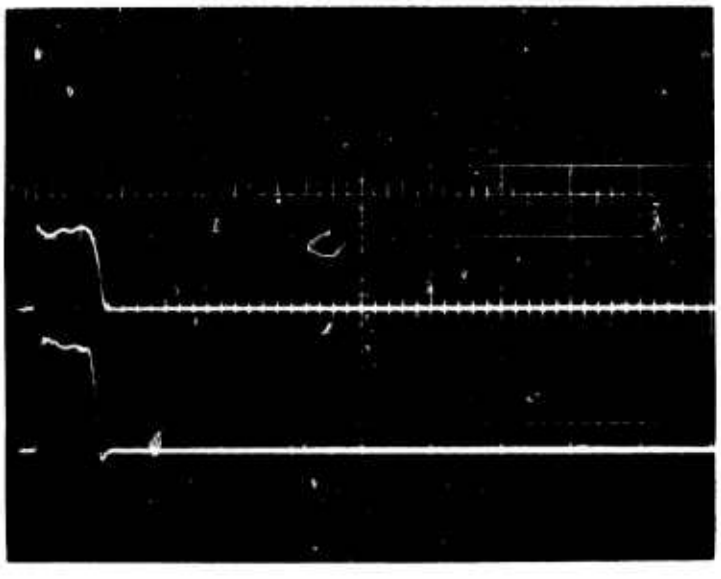

c

Diode 24-500-20-1 #4

Top: V = 100 V/division

Bottom: I = 100 mA/division

FIGURE 16

Power Output and Diode Current Under Pulsed Operation

(Horizontal scale: 1 μs/cm)

for the conventional device, under the same conditions as shown in Figure 16a. The decreasing current and increasing voltage during the duration of the pulse are results of changing I-V characteristics due to heating of the junction, and, to a lesser degree, to transient impedance changes in the diode junction.

Figures 17a and b show power output and current waveforms under slightly longer pulse conditions than in Figure 16, and differ in that the current level in Figure 17a is slightly greater than in Figure 17b. Shown here is the sharp current-dependent output power saturation characteristics. In Figure 17a, the initial value of current is higher than the optimum level. As the current decreases slightly during the pulse, the power output gradually increases. In Figure 17b, the initial value of current is also above saturation, but the final value is below saturation, so the output increases to its maximum value and then decreases during the pulse. To eliminate these effects from the measurements, a higher impedance (constant current) pulse source is needed. Circuitry for such a source is being investigated.

In the above pulsed experiments, currents of 150-200 milliamperes were used, producing current densities at RF power saturation of the order of 1600 amperes/cm^2. These very high current densities indicate uniform avalanching, which probably will result in comparatively low noise, as well as high power.

We may extrapolate these results to get an indication of the usefulness of these diodes as models of the ultimate diode we are seeking to develop. If the junction diameter were increased to 6 mils, as is planned, and the current density remained the same, then one would expect to obtain up to two watts output. An array of 5 or 6 such devices, suitably spaced diamond heat sinks, should then give approximately the required ten watts. These diodes, then, can be viewed as exemplary models, and will be studied in great detail.

IV NOISE SPECTRA OF AVALANCHE DIODE OSCILLATORS

In the previous report, FM noise measurements were described and data given for a free-running oscillator and an oscillator stabilized by means of a discriminator AFC loop. Also described was a set-up for the measurement of AM noise spectra at frequencies far removed from the carrier (Figure 11 of First Quarterly Report). During the period reported here, additional apparatus has been built to measure AM noise at frequencies close to the carrier. Figure 18 shows a block diagram of the set-up.

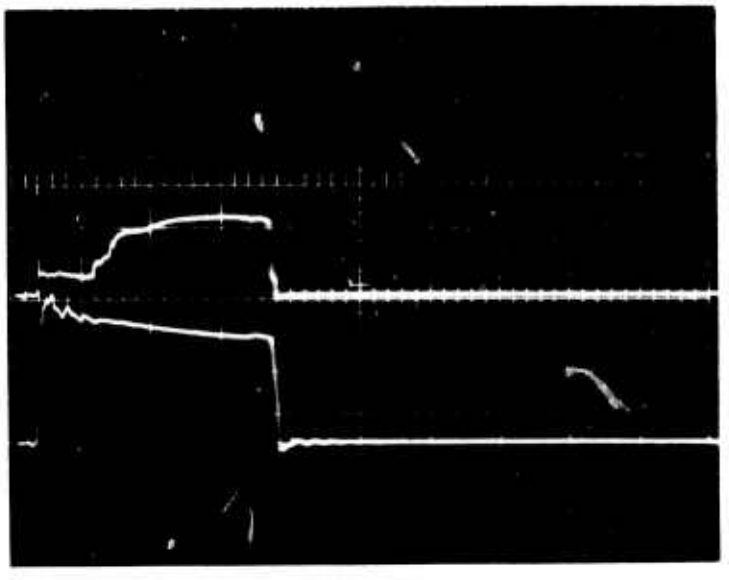

a

Diode 24-500-20-1 #4

Top: P_{out} = 1 w/division

Bottom 50 mA/division

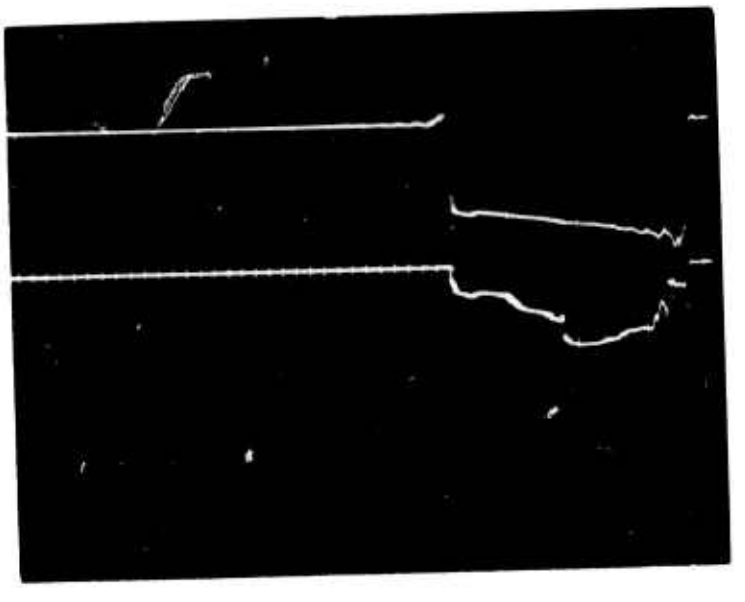

b

Diode 24-500-20-1 #4

Top: P_{out} = 1 w/division

Bottom: I = 100 mA/division

FIGURE 17

Power Output and Diode Current Under Slightly Longer Pulse Conditions Than Figure 16

(Horizontal scale: 1 μs/cm)

FIGURE 18
AM NOISE MEASURING SYSTEM

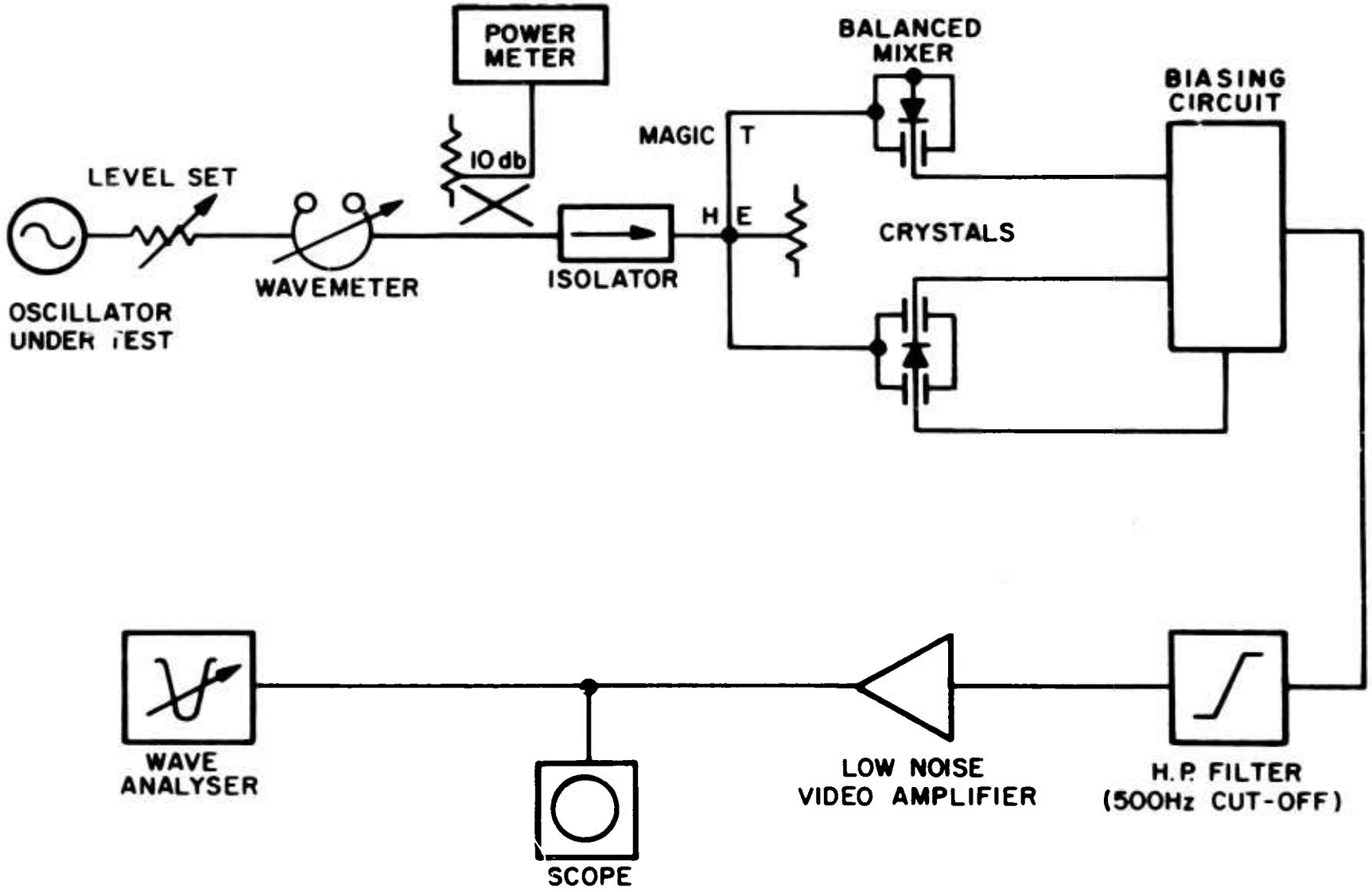

In this arrangement, a balanced mixer is used, with the carrier of the oscillator under test acting as the local oscillator, and the noise sidebands as the signals to be downconverted. The polarity of the diodes in the mixer are such that the out of phase (FM) components are cancelled. The output of the mixer is filtered, amplified, and analyzed by a frequency-selective voltmeter. Measurements down to 200 Hz have been made. Results of these measurements, in Figure 19, up to 1 GHz show that, normalized to a 1 KHz bandwidth, the noise-to-signal ratio of the oscillator tested was about 110 db up to approximately 100 MHz, then falls off at higher frequencies at 6 db/octave.

Interesting results have recently been obtained by varying the impedance of the bias circuit. In the range of 1 MHz to several hundred megahertz off carrier, significant reductions in noise could be effected by varying the bias network impedance. This work is continuing.

V WORK PLANS FOR NEXT QUARTER

1. Continue investigation of diode structures such as 24-500-20.

2. Continue optimization of chip mounting, including inverted mounting on both copper and diamond heat sinks.

3. Continue studies of device passivation.

4. Continue studies of silicon material technology.

5. Continue pulse testing of oscillators; develop constant current pulsed bias source.

6. Continue investigation of noise properties and noise reduction through bias circuit optimization.

FIGURE 19
AM NOISE TO SIGNAL RATIO FOR SILICON AVALANCHE DIODE
(NORMALIZED TO 1KHz BAND)

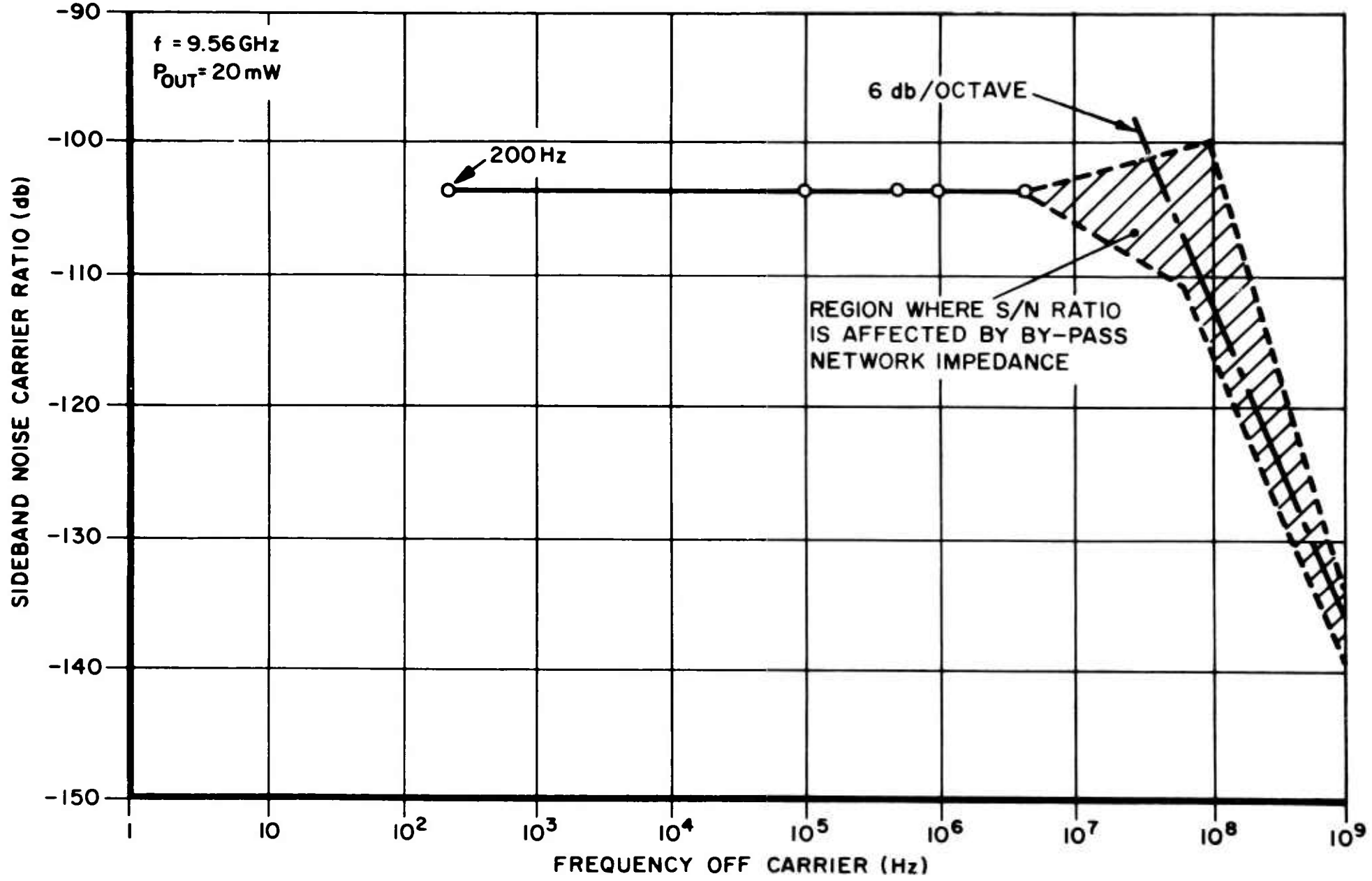

APPENDIX A

LIST OF SYMBOLS AND ABBREVIATIONS

LIST OF SYMBOLS AND ABBREVIATIONS

$\mathring{A}$	=	Angstrom unit, a unit of length equal to 1×10^{-10} meter
AFC	=	Automatic Frequency Control
AM	=	Amplitude Modulation
Ag	=	silver
As	=	arsenic
Au	=	gold
cm = Centimeter	=	1×10^{-2} meter
C-V plot	=	a graph depicting capacitance variation of a diode with change in voltage across the diode
CW	=	continuous wave
^{o}C	=	degrees centigrade, a unit of temperature
db	=	decibel
erfc	=	complementary error function
FM	=	Frequency Modulation
Hz, MHz, GHz	=	hertz, megahertz, gigahertz, units of frequency equal to one cycle per second, 1×10^{6} cps and 1×10^{9} cps, respectively.
I_F	=	current flowing through a diode in the forward direction
I_{in}	=	oscillator input current
ℓ	=	total width of depletion layer
mA	=	milliampere, a unit of electrical current equal to 10^{-3} ampere
Mo	=	molybdenum
mw, mW	=	milliwatt, a unit of electrical power equal to 10^{-3} watt
Ni	=	nickel

P	=	total heat power
P_e	=	electrical input power to heat bath (in thermal conductivity measurements)
P_h	=	heat input power to heat bath (in thermal conductivity measurements) = P_e
P_{in}	=	oscillator input power
P_{out}	=	oscillator output power
r_c	=	radius of point contact
RF	=	Radio Frequency
R_T	=	thermal resistance (expressed in degrees centigrade per watt)
r_1, r_2	=	radii as defined by Figure 6
Sb	=	antimony
T_1, T_2	=	temperatures as defined by Figure 6
T_b, T_c	=	temperature of heat bath and point contact, resp., in diamond thermal conductivity measurements
V_B	=	breakdown voltage
V_{in}	=	oscillator input voltage
W, w	=	watt, a unit of electrical power
χ	=	heat conductivity
μA	=	microampere, a unit of electrical current equal to 10^{-6} ampere
μM	=	micrometer, a unit of length equal to 10^{-6} meter
μs	=	microsecond, a unit of time equal to 10^{-6} second
% Eff.	=	percent efficiency

REFERENCE

1 "Hot-Carrier Microwave Detector," R Harrison and J. Zucker, Proc. of the IEEE, Vol. 54, No. 4, April 1966, pp. 588-595.

Security Classification

DOCUMENT CONTROL DATA · R&D

(Security classification of title, body of abstract and indexing annotation must be entered when the overall report is classified)

1. ORIGINATING ACTIVITY (Corporate author) Sylvania Electric Products, Inc. SEMICONDUCTOR DIVISION 100 Sylvan Road, Woburn, Massachusetts 01801	2a. REPORT SECURITY CLASSIFICATION UNCLASSIFIED 2b. GROUP DNA

3. REPORT TITLE

"MICROWAVE GENERATION FROM AVALANCHE TRANSIT TIME DIODES"

4. DESCRIPTIVE NOTES (Type of report and inclusive dates)

Second Quarterly Report - 1 October 1967 to 31 December 1967

5. AUTHOR(S) (Last name, first name, initial)

SOLOMON, Arthur H., Levi, Clifford; and Scherer, Ernst

6. REPORT DATE	7a. TOTAL NO. OF PAGES	7b. NO. OF REFS
April, 1968	35	1

8a. CONTRACT OR GRANT NO.	9a. ORIGINATOR'S REPORT NUMBER(S)
DAAB07-67-C-0671 b. PROJECT NO. DA Project No. 7910.21.243.38 c. d.	9b. OTHER REPORT NO(S) (Any other numbers that may be assigned this report) ECOM-0671-2

10. AVAILABILITY/LIMITATION NOTICES This document is subject to export controls and each transmittal to foreign government or foreign nationals may be made only with prior approval of CG, U. S. Army Electronics Command, Fort Monmouth, N. J. Attn: AMSEL-KL-SM

11. SUPPLEMENTARY NOTES	12. SPONSORING MILITARY ACTIVITY
ARPA Order No. 692	U. S. Army Electronics Command Ft. Monmouth, New Jersey 07703 (AMSEL-KL-SM)

13. ABSTRACT Work during the second quarter was devoted to device geometry optimization, inverted chip mounting, diamond heat sink classification and evaluation of noise characteristics. While inverted chip mounting was effective in reducing thermal resistance, oscillator efficiency was lower than that obtained from similar devices conventionally mounted. Several possible reasons for the poor RF performance of inverted chip diodes are being investigated. However, conventionally-mounted devices were pulse tested and over 1 watt of peak pulse power was obtained at 8.6 GHz, with 7 percent efficiency. These diodes are being studied as models of desired characteristics in inverted mount devices. Noise measurements on various diodes indicate that AM noise is essentially constant from about 100 MHz off carrier down to 200 Hz off carrier, which is as close to the carrier as measurements could be made. The sideband noise-to-carrier ratio was about -105 db in a 1 KHz bandwidth, in an oscillator cavity having a loaded Q of about 100.

DD FORM 1 JAN 64 1473

Security Classification

14. KEY WORDS	LINK A		LINK B		LINK C	
	ROLE	WT	ROLE	WT	ROLE	WT
Avalanche Diode						
Microwave Oscillator						
Silicon						
A. M. Noise						
Thermal Resistance						
Infrared Spectra						
Ion Implantation						

INSTRUCTIONS

1. ORIGINATING ACTIVITY: Enter the name and address of the contractor, subcontractor, grantee, Department of Defense activity or other organization *(corporate author)* issuing the report.

2a. REPORT SECURITY CLASSIFICATION: Enter the overall security classificstion of the report. Indicate whether "Restricted Data" is included. Marking is to be in accordance with appropriate security regulations.

2b. GROUP: Automatic downgrading is specified in DoD Directive 5200.10 and Armed Forces Industrial Manual. Enter the group number. Also, when applicable, show that optional markings have been used for Group 3 and Group 4 as authorized.

3. REPORT TITLE: Enter the complete report title in all capital letters. Titles in all cases should be unclassified. If a meaningful title cannot be selected without classification, show title classification in all capitals in parenthesis immediately following the title.

4. DESCRIPTIVE NOTES: If appropriate, enter the type of report, e.g., interim, progress, summary, annual, or final. Give the inclusive dates when a specific reporting period is covered.

5. AUTHOR(S): Enter the name(s) of author(s) as shown on or in the report. Enter last name, first name, middle initial. If military, show rank and branch of service. The name of the principal author is an absolute minimum requirement.

6. REPORT DATE: Enter the date of the report as day, month, year; or month, year. If more than one date appears on the report, use date of publication.

7a. TOTAL NUMBER OF PAGES: The total page count should follow normal pagination procedures, i.e., enter the number of pages containing information.

7b. NUMBER OF REFERENCES: Enter the total number of references cited in the report.

8a. CONTRACT OR GRANT NUMBER: If appropriate, enter the applicable number of the contract or grant under which the report was written.

8b, 8c, & 8d. PROJECT NUMBER: Enter the appropriate military department identification, such as project number, subproject number, system numbers, task number, etc.

9a. ORIGINATOR'S REPORT NUMBER(S): Enter the official report number by which the document will be identified and controlled by the originating activity. This number must be unique to this report.

9b. OTHER REPORT NUMBER(S): If the report has been assigned any other report numbers *(either by the originator or by the sponsor)*, also enter this number(s).

10. AVAILABILITY/LIMITATION NOTICES: Enter any limitations on further dissemination of the report, other than those imposed by security classification, using standard statements such as:

(1) "Qualified requesters may obtain copies of this report from DDC."

(2) "Foreign announcement and dissemination of this report by DDC is not authorized."

(3) "U. S. Government agencies may obtain copies of this report directly from DDC. Other qualified DDC users shall request through _____."

(4) "U. S. military agencies may obtain copies of this report directly from DDC. Other qualified users shall request through _____."

(5) "All distribution of this report is controlled. Qualified DDC users shall request through _____."

If the report has been furnished to the Office of Technical Services, Department of Commerce, for sale to the public, indicate this fact and enter the price, if known.

11. SUPPLEMENTARY NOTES: Use for additional explanatory notes.

12. SPONSORING MILITARY ACTIVITY: Enter the name of the departmental project office or laboratory sponsoring *(paying for)* the research and development. Include address.

13. ABSTRACT: Enter an abstract giving a brief and factual summary of the document indicative of the report, even though it may also appear elsewhere in the body of the technical report. If additional space is required, a continuation sheet shall be attached.

It is highly desirable that the abstract of classified reports be unclassified. Each paragraph of the abstract shall end with an indication of the military security classification of the information in the paragraph, represented as *(TS)*, *(S)*, *(C)*, or *(U)*.

There is no limitation on the length of the abstract. However, the suggested length is from 150 to 225 words.

14. KEY WORDS: Key words are technically meaningful terms or short phrases that characterize a report and may be used as index entries for cataloging the report. Key words must be selected so that no security classification is required. Identifiers, such as equipment model designation, trade name, military project code name, geographic location, may be used as key words but will be followed by an indication of technical context. The assignment of links, rules, and weights is optional.